# Statistical Skin-Return Results for Retrodirective Cross-Eye Jamming

W. P. du Plessis, *Senior Member, IEEE*

*Abstract*—The effect of the return from the platform on which a cross-eye jammer is mounted is significant in many practical cross-eye jamming scenarios. However, all published analyses of skin-return affected cross-eye jamming have significant limitations. These limitations are addressed by deriving equations for the distribution of the cross-eye gain in the presence of skin return. The value of these results is demonstrated by using them to gain insight into how skin return affects cross-eye jamming.

*Index Terms*—Cross-eye jamming, electronic warfare (EW), electronic countermeasures (ECM), radar countermeasures, and monopulse radar.

W. P. du Plessis is with the University of Pretoria, Pretoria, 0002, South Africa (e-mail: wduplessis@ieee.org).

## I. INTRODUCTION

Cross-eye jamming attempts to induce an angular error in a threat radar by recreating the worst-case error due to glint [1]–[8]. The fact that glint is a naturally-occurring phenomenon makes cross-eye jamming extremely attractive as it is capable of affecting all radar systems.

Cross-eye jamming relies on transmitting two signals which have similar amplitudes and a phase difference of approximately 180° from antennas which are separated by a large distance known as the baseline (10 m to 20 m being typical [7]). While many potential implementations of cross-eye jamming exist, the retrodirective implementation appears to be the only way to reduce the tolerance requirements of a cross-eye jammer to achievable levels [2], [4], [5], [8]. Retrodirective cross-eye jamming is based on a Van-Atta array [9], with the signal received by the antenna on one side of the jammer is retransmitted from the antenna on the other side of the jammer and vice versa.

The phase-front analysis of glint has traditionally been applied to cross-eye jamming, but the results obtained have been shown to be inaccurate when applied to retrodirective cross-eye jamming [8], [10], [11]. As outlined above, the implementation of practical cross-eye jammers does not appear to be possible without using the retrodirective implementation, so this is a significant limitation of the phase-front analysis.

It may not always be possible to isolate the return of a cross-eye jammer from the return of the platform on which the jammer is mounted (the platform skin return), so the case where both platform skin return and jammer returns are simultaneously received by the threat radar is important. While some considerations of this case have appeared in the literature, they fall into one of two categories. The first group merely states that a high jammer-to-signal ratio (JSR) (often stated as 20 dB) is required without providing any analysis to support this statement [2], [4]–[6], [12]. The second group performs detailed analyses, but as with most cross-eye jamming analyses, neglects the retrodirective implementation [1], [3], [13], [14], leading to significant errors [15].

While an analysis of retrodirective cross-eye jamming the presence of platform skin return has been published [15], it lacks mathematical rigour. Most importantly, the result derived in the appendix of [15] claims that

$$\text{median} \left[ \frac{k_1 + k_2 \cos(\phi_s) + k_3 \sin(\phi_s)}{k_4 + k_5 \cos(\phi_s) + k_6 \sin(\phi_s)} \right] = \frac{k_1}{k_4} \quad (1)$$

when $\phi_s$ is uniformly distributed over all angles. However, this result can be proved to be incorrect in the

general case by setting $k_n = n$ and computing the distribution of the result numerically using $10^6$ values of $\phi_s$ uniformly distributed over the range $[0, 2\pi)$ to obtain a median value of 0.3909 rather than the value of 0.2500 predicted by (1). The distribution of the $f$ used in the derivation of the median is obviously also not valid except in special cases. There is thus a need to confirm whether the results presented in [15] are accurate.

Additionally, the published results for skin-return affected retrodirective cross-eye jamming are limited by the fact that they only consider certain specific results rather than the complete general case. For example, only the median cross-eye gain is considered in detail in [15], and only the JSR required to limit a target to one side of the jammer is provided in [16]. The extremely large variations that are possible in the presence of platform skin return [15] mean that these specific results provide only a limited description of the complete problem.

The limitations of existing published analyses are addressed by providing a mathematically-rigorous derivation of the distribution of the cross-eye gain obtained when a cross-eye jammer is operated in the presence of platform skin return. The mathematical rigour allows the results to be used with confidence, while the fact the full distribution is available allows a number of cases which could not be considered previously to be evaluated. An extensive discussion of the results is presented to provide insight into the functioning of a retrodirective cross-eye jammer in the presence of platform skin return.

Section II provides a summary of previously-published work, and Section III then uses this background to derive equations for the cross-eye gain distribution. A number of examples of how the results derived can be used are provided in Section IV along with a discussion of the implications of each result. Finally, a brief conclusion is provided in Section V.

## II. SUMMARY OF PREVIOUS RESULTS

The analysis of cross-eye jamming in the presence of platform skin return in [15] is briefly summarised below as it provides the basis for the present work.

The estimate of the angle to a target, the indicated angle, for a phase-comparison monopulse system can be computed from the monopulse ratio using [17]

$$M = \tan\left[\beta \frac{d_r}{2} \sin(\theta_i)\right] \qquad (2)$$

where $M$ is the monopulse ratio, $\theta_i$ is the monopulse indicated angle, $\beta$ is the free-space propagation factor, and $d_r$ is the spacing of the phase-comparison radar antennas as shown in Fig. 1. While only phase-comparison
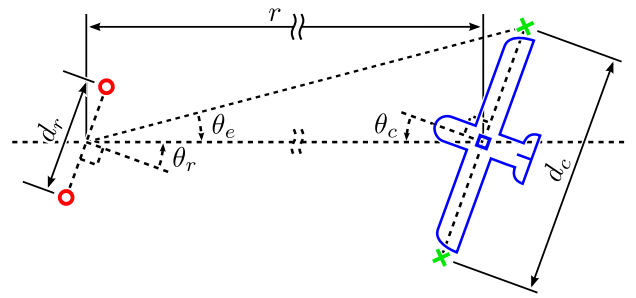


Fig. 1. The geometry of the cross-eye jamming scenario which includes the effect of platform skin return [15]. The phase centres of the phase-comparison monopulse radar antennas and the jammer antennas are denoted by circles and crosses respectively, and the point target used to model the platform skin return is denoted by a square.
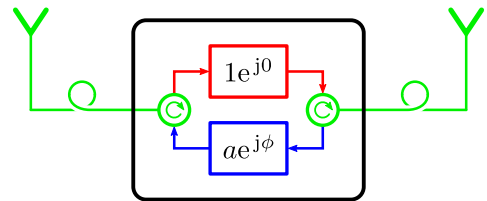


Fig. 2. The retrodirective implementation of a cross-eye jammer showing the definition of $a$ and $\phi$.

monopulse is considered, the results have been shown to be valid for all monopulse systems [8], [18].

The monopulse ratio received from a retrodirective cross-eye jammer mounted on a platform whose return (the platform skin return) is modelled by a point scatterer halfway between the jammer antennas is given by

$$M_t \approx \tan(k) + G_{Ct} \frac{\sin(2k_c)}{\cos(2k) + 1} \qquad (3)$$

where

$$k \approx \beta \frac{d_r}{2} \sin(\theta_r) \qquad (4)$$

$$k_c \approx \beta \frac{d_r}{2} \cos(\theta_r) \theta_e \qquad (5)$$

$$\theta_e \approx \frac{d_c}{2r} \cos(\theta_c) \qquad (6)$$

with the geometrical parameters being defined in Fig. 1.

The cross-eye gain is a figure of merit which can be used to quantify the performance of a cross-eye jammer. The total cross-eye gain including the effect of platform skin return is given by

$$G_{Ct} = \mathcal{R}e\left\{\frac{1 - ae^{j\phi}}{1 + ae^{j\phi} + a_s e^{j\phi_s}}\right\} \qquad (7)$$

where $a$ and $\phi$ are the relative gain and phase shift of the two directions through the retrodirective cross-eye jammer as shown in Fig. 2.

The effect of platform skin return is included via the parameters $a_s$ and $\phi_s$, which are defined as the amplitude

and phase of the skin return relative to the stronger of the two jammer signals (i.e. relative to the jammer when $a = 0$). The value of $a_s$ is related to the JSR by

$$\text{JSR} = \frac{1}{a_s^2} \tag{8}$$

with the gain of the cross-eye jammer and its antennas being incorporated into $a_s$.

The result in (8) implicitly means that $a \leq 1$ because JSR is defined as the skin return relative to the stronger of the two jammer-channel returns. Results obtained using $a = x$ are identical to results obtained for $a = 1/x$ except that the apparent target is produced on the opposite side of the jammer (the sign of the cross-eye gain is inverted), so limiting the range of $a$ does not affect the generality of the results [8], [19].

The median value of the total cross-eye gain has been shown to be

$$G_{Ctm} = \frac{1 - a^2}{1 + a^2 + 2a\cos(\phi) + a_s^2}, \tag{9}$$

and while the derivation of this result in [15] had errors, (9) is shown to be correct in Section III.

The apparent target created by a cross-eye jammer is limited to one side of the jammer when total cross-eye gain is strictly positive ($G_{Ct} \geq 0$) giving [16]

$$a_s < \frac{1 - a^2}{\sqrt{1 + a^2 - 2a\cos(\phi)}} \tag{10}$$

$$\text{JSR} > \frac{1 + a^2 - 2a\cos(\phi)}{(1 - a^2)^2} \tag{11}$$

where (8) was used to convert $a_s$ to JSR.

The monopulse ratio in (3) includes a number of approximations which are briefly summarised below.

1) The approximate forms of $k$, $k_c$ and $\theta_e$ in (4) to (6) are extremely accurate for practical cross-eye jamming scenarios [8].
2) The gains of the two radar antenna elements in the directions of the jammer antenna elements are assumed to be identical.

$$P_r\left(\theta_r - \theta_e\right)P_r\left(\theta_r + \theta_e\right) \approx \left[P_r\left(\theta_r\right)\right]^2 \tag{12}$$

This is reasonable as the radar antenna pattern is predominantly determined by the spacing of the radar antenna elements.

3) The gains of the two jammer antenna elements in the directions of the radar are assumed to be identical.

$$P_c\left(\theta_c - \theta_e\right)P_c\left(\theta_c + \theta_e\right) \approx \left[P_c\left(\theta_c\right)\right]^2 \approx 1 \tag{13}$$

The main effect of this assumption is to change the JSR, but as outlined above, the jammer-antenna gain is assumed to be included in $a_s$.

4) The following approximation

$$\cos\left(2k_c\right) \approx 1 \tag{14}$$

is accurate. This is the least accurate of the approximations and will dominate the error.

Approximation 4 is accurate under the conditions listed below.

- The jammer antenna separation seen by the radar is small as a small value of $\theta_e$ leads to a small value of $k_c$. This condition is achieved as the radar must not be able to resolve the jammer antennas for cross-eye jamming to be effective [10].
- The jammer is far from the first null of the radar sum-channel beamwidth where the radar antenna-element patterns change rapidly. This condition should be satisfied as radar is unlikely to track targets far outside the 3-dB beamwidth of its sum-channel beam.
- The total sum-channel return is large. Violating this condition leads to large, uncontrollable variations in the cross-eye gain, which leads to many practical difficulties in effectively employing cross-eye jamming. This condition is thus unlikely to be of interest to practical cross-eye jammer systems.

## III. ANALYSIS

The derivation of the distribution of the total cross-eye gain is first provided, followed by the development of simplified results for the extreme values of the total cross-eye gain.

As the phase of the skin return relative to the jammer return $\phi_s$ cannot be specified or determined with any certainty, the cross-eye gain is a distribution rather than a single value [15]. The median total cross-eye gain and the proportion of the total cross-eye gain values which are on the opposite side of the jammer to the intended target have been considered previously [15], [16], so the analysis below focuses on extending the results to obtain closed-form solutions of the distribution of the total cross-eye gain.

The total cross-eye gain in (7) can be expanded to

$$
\begin{aligned}
G_{Ct} &= \frac{1 - a^2 + a_s\cos(\phi_s) - \cdots}{1 + a^2 + a_s^2 + 2a\cos(\phi) + \cdots} \\
&\quad \frac{\cdots aa_s\cos(\phi_s - \phi)}{\cdots 2a_s\cos(\phi_s) + 2aa_s\cos(\phi_s - \phi)} \\
&= \frac{1 - a^2 + \cdots}{1 + a^2 + a_s^2 + 2a\cos(\phi) + \cdots} \\
&\quad \frac{\cdots a_s\left[1 - a\cos(\phi)\right]\cos(\phi_s) - \cdots}{\cdots 2a_s\left[1 + a\cos(\phi)\right]\cos(\phi_s) + \cdots}
\end{aligned}
\tag{15}
$$

$$\frac{\cdots aa_s \sin(\phi)\sin(\phi_s)}{\cdots 2aa_s \sin(\phi)\sin(\phi_s)} \tag{16}$$

$$= \frac{k_1 + k_2 \cos(\phi_s) + k_3 \sin(\phi_s)}{k_4 + k_5 \cos(\phi_s) + k_6 \sin(\phi_s)} \tag{17}$$

where

$$k_1 = 1 - a^2 \tag{18}$$
$$k_2 = a_s \left[1 - a\cos(\phi)\right] \tag{19}$$
$$k_3 = -a_s a \sin(\phi) \tag{20}$$
$$k_4 = 1 + a^2 + 2a\cos(\phi) + a_s^2 \tag{21}$$
$$k_5 = 2a_s \left[1 + a\cos(\phi)\right] \tag{22}$$
$$k_6 = 2a_s a \sin(\phi) \tag{23}$$

of which only $k_3$ and $k_6$ can be negative because $0 \leq a \leq 1$ and $a_s \geq 0$.

Equation (17) can be rewritten as

$$0 = (k_1 - G_{Ct}k_4) + (k_2 - G_{Ct}k_5)\cos(\phi_s) + \\ (k_3 - G_{Ct}k_6)\sin(\phi_s) \tag{24}$$

$$= (k_1 - G_{Ct}k_4) + \\ k_m \left[\cos(\theta)\cos(\phi_s) + \sin(\theta)\sin(\phi_s)\right] \tag{25}$$

$$= (k_1 - G_{Ct}k_4) + k_m \cos(\phi_s - \theta) \tag{26}$$

$$= (k_1 - G_{Ct}k_4) + k_m \cos(x) \tag{27}$$

$$\cos(x) = \frac{G_{Ct}k_4 - k_1}{k_m} \tag{28}$$

where

$$\cos(\theta) = \frac{k_2 - G_{Ct}k_5}{k_m} \tag{29}$$

$$\sin(\theta) = \frac{k_3 - G_{Ct}k_6}{k_m} \tag{30}$$

$$k_m^2 = (k_2 - G_{Ct}k_5)^2 + (k_3 - G_{Ct}k_6)^2 \tag{31}$$

$$= a_s^2 \left[(2G_{Ct} - 1)^2 + a^2(2G_{Ct} + 1)^2 + \\ 2a\cos(\phi)(2G_{Ct} - 1)(2G_{Ct} + 1)\right] \tag{32}$$

with $k_m \geq 0$ as it is a magnitude, and

$$x = \phi_s - \theta. \tag{33}$$

The variable $x$ can take any angle with equal probability because $\theta$ is a constant and $\phi_s$ is uniformly distributed over all angles.

Equation (28) can now be used to determine the cumulative distribution of $G_{Ct}$ from the cumulative distribution of $x$. However, this process is predicated on (28) having a one-to-one relationship between $\cos(x)$ and $G_{Ct}$. It will firstly be shown that the right-hand side (RHS) of (28) is monotonic (i.e. each value only occurs once), after which the fact that each value of $\cos(x)$ corresponds to multiple values of $x$ will be addressed.

The first step to showing that the RHS of (28) is monotonic is demonstrating that its derivative can only be zero for values of $G_{Ct}$ which make the magnitude of the RHS of (28) greater than 1. Such values are outside the allowable range of the left-hand side (LHS) of (28) because $|\cos(x)| \leq 1$, thereby ensuring that it is not possible for the gradient of the RHS of (28) to change sign within the allowable range of values. As the gradient cannot change sign, it is impossible for the same value to be obtained twice.[1]

The derivative of (28) with respect to $G_{Ct}$ is zero when

$$0 = \frac{\partial}{\partial G_{Ct}} \frac{G_{Ct}k_4 - k_1}{k_m} \tag{34}$$

$$= \frac{k_4}{k_m} + \frac{(G_{Ct}k_4 - k_1)}{k_m^3} \times \\ \left[k_6(k_3 - G_{Ct}k_6) + k_5(k_2 - G_{Ct}k_5)\right] \tag{35}$$

$$G_{Ct} = \frac{k_2(k_1k_5 - k_2k_4) + k_3(k_1k_6 - k_3k_4)}{k_5(k_1k_5 - k_2k_4) + k_6(k_1k_6 - k_3k_4)}. \tag{36}$$

Substituting this value of $G_{Ct}$ into (28), squaring the result and simplifying gives

$$\cos^2(x) = \frac{(k_1k_6 - k_3k_4)^2 + (k_1k_5 - k_2k_4)^2}{(k_2k_6 - k_3k_5)^2}. \tag{37}$$

Ensuring that the RHS of (37) is greater than the maximum possible value of the LHS, gives the general requirement for a monotonic result as

$$1 < \frac{(k_1k_6 - k_3k_4)^2 + (k_1k_5 - k_2k_4)^2}{(k_2k_6 - k_3k_5)^2} \tag{38}$$

$$0 < (k_1k_6 - k_3k_4)^2 + (k_1k_5 - k_2k_4)^2 - \\ (k_2k_6 - k_3k_5)^2. \tag{39}$$

For the cross-eye jamming case, (39) becomes

$$a_s^2 \left[1 + a^2 - 2a\cos(\phi)\right] \times \\ \left[1 + a^2 + 2a\cos(\phi) - a_s^2\right]^2 > 0 \tag{40}$$

where none of the factors can be negative because $a < 1$.

However, the derivation of the general case in (36) requires multiplication by $k_m^3$ causing the LHS to take the form $0 \cdot \infty$ when $k_m \to \pm\infty$. This situation is possible as the value of $k_m$ will become infinite when the cross-eye gain is infinite ($G_{Ct} \to \infty$). Additionally, the value of the RHS of (28) takes the form $\infty/\infty$ when $k_m$ is infinite. Finally, the value of (40) can be zero when

[1]Note that this approach is slightly conservative as an inflection point (derivative is zero but does not change sign) within the range $[-1, 1]$ would also produce a monotonic gradient. However, the analysis of this case is more complex, and the more conservative result is adequate for the case considered here.

the cross-eye gain is infinite because the third factor of the LHS of (40) is zero when the magnitudes of the sum-channel jammer and skin returns are equal as required for infinite cross-eye gain (see (43) and (44) below).[2] The second step in proving that the RHS of (28) is monotonic thus requires demonstrating that the RHS of (28) tends to $\pm 1$ (the extreme values of the LHS of (28)) as $G_{Ct} \to \pm\infty$ (the extreme values of the RHS of (28)) when infinite cross-eye gain is possible.

Using L'Hôpital's Rule [20], it can be shown that

$$\lim_{G_{Ct} \to \pm\infty} \frac{G_{Ct}k_4 - k_1}{k_m} = \pm \frac{k_4}{\sqrt{k_5^2 + k_6^2}} \qquad (41)$$

$$= \pm \frac{1 + a^2 + 2a\cos(\phi) + a_s^2}{2a_s\sqrt{1 + a^2 + 2a\cos(\phi)}}. \qquad (42)$$

In the general case, $|k_4| \geq \sqrt{k_5^2 + k_6^2}$ will either avoid an infinite result by ensuring that the denominator of (17) is never zero or ensure that (41) holds. In the cross-eye jamming case, the only way to obtain an infinite cross-eye gain is if the denominator of (7) is zero, giving

$$\left| 1 + ae^{j\phi} \right| = \left| a_s e^{j\phi_s} \right| \qquad (43)$$

$$\sqrt{1 + a^2 + 2a\cos(\phi)} = a_s \qquad (44)$$

because $a_s \geq 0$, and substituting (44) into (42) gives

$$\lim_{G_{Ct} \to \pm\infty} \frac{G_{Ct}k_4 - k_1}{k_m} = \pm 1 \qquad (45)$$

as required.

The required monotonicity of the RHS of (28) thus exists in the general case when

$$(k_1 k_6 - k_3 k_4)^2 + (k_1 k_5 - k_2 k_4)^2 - \\ (k_2 k_6 - k_3 k_5)^2 > 0 \quad (46)$$

and

$$|k_4| \geq \sqrt{k_5^2 + k_6^2}. \qquad (47)$$

For cross-eye jamming, the first condition will always be satisfied, except when the cross-eye gain is infinite ($G_{Ct} \to \pm\infty$), but the second condition addresses this case. Furthermore, the first condition is only violated at the extreme edges of the distribution, so the gradient cannot change sign within the allowable range of values. The required monotonicity of the RHS of will thus always exist (28) for retrodirective cross-eye jamming

---

in the presence of platform skin return as a result of the forms of $k_n$ in (18) to (23).

The periodic nature of the cosine function means that the cumulative distribution function of $x$ can be bounded by any values as long as a full $2\pi$ range of angles is covered. The cumulative distribution function

$$F_x(x) = \begin{cases} 0 & x \leq -\pi \\ \frac{1}{2\pi}(x + \pi) & -\pi < x < \pi \\ 1 & x \geq \pi \end{cases} \qquad (48)$$

is convenient as it allows the fact that $\cos(x) = \cos(-x)$ to be exploited to resolve the difficulty that each value of the RHS of (28) corresponds to two values of $x$.

The cumulative distribution of the cross-eye gain can now be written as

$$F_{G_{Ct}}(G_{Cts}) = P\{G_{Ct} \leq G_{Cts}\} \qquad (49)$$

$$= P\{|x| \geq x_s\} \text{ or } P\{|x| \leq x_s\} \quad (50)$$

$$= P\{x \geq x_s\} + P\{x \leq -x_s\} \text{ or } \\ P\{x \leq x_s\} - P\{x \leq -x_s\} \quad (51)$$

$$= [1 - F_x(x_s)] + F_x(-x_s) \text{ or } \\ F_x(x_s) - F_x(-x_s) \quad (52)$$

$$= 1 - \frac{x_s}{\pi} \text{ or } \frac{x_s}{\pi} \qquad (53)$$

$$\pi - \pi F_{G_{Ct}} = \arccos\left(\frac{G_{Ct}k_4 - k_1}{k_m}\right) \text{ or }$$

$$\pi F_{G_{Ct}} = \arccos\left(\frac{G_{Ct}k_4 - k_1}{k_m}\right) \qquad (54)$$

$$\cos(\pi F_{G_{Ct}}) \overset{?}{=} \pm \frac{k_1 - G_{Ct}k_4}{k_m} \qquad (55)$$

where $x_s$ is the value of $x$ which corresponds to the specified value of $G_{Ct}$ denoted $G_{Cts}$. Two possible solutions are provided at each step as it is not yet clear whether the RHS of (28) increases or decreases with $G_{Ct}$.

Regardless of which form of (55) is correct, the median cross-eye gain ($G_{Ctm}$) can be shown to be

$$G_{Ctm} = \frac{k_1}{k_4} \qquad (56)$$

by setting $F_{G_{Ct}} = 0.5$ to make the LHS of (55) zero in both cases. Using $k_1$ in (18) and $k_4$ in (21) shows that (56) is identical to (9), thereby confirming that the median result presented in [15] is correct.[3]

---

Substituting the median total cross-eye gain in (56) into the RHS of (35) gives

$$\frac{\partial}{\partial G_{Ct}} \left. \frac{G_{Ct}k_4 - k_1}{k_m} \right|_{G_{Ct}=G_{Ctm}} = \frac{k_4 \, |k_4|}{\sqrt{(k_1 k_6 - k_3 k_4)^2 + (k_1 k_5 - k_2 k_4)^2}} \quad (57)$$

which has the same sign as $k_4$ in the general case. In the cross-eye jamming case, $k_4 \geq 0$, so the RHS of (28) is an increasing function of $G_{Ct}$. The cumulative distribution of the total cross-eye gain is thus given by

$$F_{G_{Ct}}(G_{Cts}) = \frac{1}{\pi} \arccos \left[ \frac{k_1 - G_{Cts}k_4}{k_m} \right]. \quad (58)$$

However, (58) produces complex results when computed using values of $G_{Cts}$ which are outside the allowable range of $G_{Ct}$ values. Fortunately, the nature of the arccosine function is such that the resulting values of $F_{G_{Ct}}(G_{Cts})$ are of the form $0+jx$ and $1+jx$ when $G_{Cts} < \min(G_{Ct})$ and $G_{Cts} > \max(G_{Ct})$ respectively, where $x$ is an arbitrary constant. A more useful form of the required cumulative distribution is thus given by

$$F_{G_{Ct}}(G_{Cts}) = \mathscr{R}e\left\{ \frac{1}{\pi} \arccos \left[ \frac{k_1 - G_{Cts}k_4}{k_m} \right] \right\} \quad (59)$$

as this form gives the desired values of 0 when $G_{Cts} < \min(G_{Ct})$ and 1 when $G_{Cts} > \max(G_{Ct})$.

Determining the value of $F_{G_{Ct}}(G_{Ct})$ using (59) allows the probability of the total cross-eye gain being lower than a specified value to be computed. However, the ability to determine the total cross-eye gain for a specified value of $F_{G_{Ct}}(G_{Ct})$ is more useful in many situations. Defining

$$k_F = -\cos\left[\pi F_{G_{Ct}}(G_{Ct})\right] \quad (60)$$

allows (59) to be rewritten as

$$k_F = \frac{G_{Ct}k_4 - k_1}{k_m} \quad (61)$$

$$k_F^2 = \frac{(G_{Ct}k_4 - k_1)^2}{(k_2 - G_{Ct}k_5)^2 + (k_3 - G_{Ct}k_6)^2} \quad (62)$$

$$0 = G_{Ct}^2 \left[k_4^2 - k_F^2 \left(k_5^2 + k_6^2\right)\right] - 2G_{Ct}\left[k_1 k_4 - k_F^2 \left(k_2 k_5 + k_3 k_6\right)\right] + \left[k_1^2 - k_F^2 \left(k_2^2 + k_3^2\right)\right]. \quad (63)$$

The solution to (63) is given by

$$G_{Ct} = \frac{k_1 k_4 - k_F^2 \left(k_2 k_5 + k_3 k_6\right) + k_F \sqrt{k_\Delta}}{k_4^2 - k_F^2 \left(k_5^2 + k_6^2\right)} \quad (64)$$

where

$$k_\Delta = (k_1 k_6 - k_3 k_4)^2 + (k_1 k_5 - k_2 k_4)^2 - k_F^2 \left(k_2 k_6 - k_3 k_5\right)^2 \quad (65)$$

was used to simplify the notation. The sign of the square-root term in the numerator of (64) could be positive or negative based on the quadratic solution to (63), but only the positive sign is valid here. This may be shown by noting that the RHS of (61) is strictly increasing as demonstrated previously for (28), so $G_{Ct}$ must increase as $k_F$ increases.

The extreme values of $G_{Ct}$ may be obtained from (28) by finding the values of $G_{Ct}$ with correspond to the extreme values of the LHS of (28) as follows

$$1 = \left| \frac{G_{Ctx}k_4 - k_1}{k_m} \right| \quad (66)$$

$$k_m^2 = (G_{Ctx}k_4 - k_1)^2 \quad (67)$$

$$G_{Ctx} = \frac{1 - a^2 \pm a_s \sqrt{1 + a^2 - 2a\cos(\phi)}}{1 + a^2 + 2a\cos(\phi) - a_s^2} \quad (68)$$

where $G_{Ctx}$ denotes the extreme values of $G_{Ct}$. Determining which of the $G_{Ctx}$ values in (68) correspond to the minimum and maximum values of $G_{Ct}$ requires both the sign of the denominator and the sign of the numerator term which can be added or subtracted to be considered.

The first portion of the denominator of (68) corresponds to the magnitude of the total sum-channel jammer return [15], [16] and thus cannot be negative.

$$1 + a^2 + 2a\cos(\phi) = \left|1 + ae^{j\phi}\right|^2 \geq 0 \quad (69)$$

Furthermore, a non-zero total jammer return ($a \neq 1$) has been shown to reduce the effect of tolerances [1], [3], [8], [19] and of platform skin return [15], so the value of (69) will be greater than zero in practical systems. The denominator of (68) is only zero when

$$a_s^2 = 1 + a^2 + 2a\cos(\phi) \quad (70)$$

which corresponds to

$$\mathrm{JSR}_c = \frac{1}{1 + a^2 + 2a\cos(\phi)}. \quad (71)$$

This is the critical value of the JSR (denoted $\mathrm{JSR}_c$) where the skin return and the total jammer sum-channel return are equal. The sign of the denominator is negative when the JSR is below $\mathrm{JSR}_c$ and positive above $\mathrm{JSR}_c$. The minimum value of $G_{Ct}$ is thus obtained from (68) when $\pm \rightarrow -$ and $\mathrm{JSR} > \mathrm{JSR}_c$, and when $\pm \rightarrow +$ and $\mathrm{JSR} < \mathrm{JSR}_c$. The opposite sign of the $\pm$ corresponds to the maximum value of $G_{Ct}$ in each case.

The value of $\mathrm{JSR}_c$ is also significant because both the minimum and maximum values of $G_{Ct}$ at this point are

infinite, so the largest variation in $G_{Ct}$ is obtained at $JSR_c$. This is a result of the fact that the cancellation of the jammer and skin returns make the denominator of $G_{Ct}$ in (7) equal to zero.

When (70) is substituted into (9) the median total cross-eye gain becomes

$$G_{Ctm} = \frac{1 - a^2}{2\left[1 + a^2 + 2a\cos(\phi)\right]} \qquad (72)$$

$$= \frac{1}{2}G_C \qquad \text{when JSR = } JSR_c \qquad (73)$$

which shows that the median total cross-eye gain is half the cross-eye gain in the absence of platform skin return [6], [8]

$$G_C = \frac{1 - a^2}{1 + a^2 + 2a\cos(\phi)} \qquad (74)$$

when the JSR is $JSR_c$. This result agrees with previously-published work where a JSR of the form (71) is shown to produce $G_{Ctm} = 0.5G_C$ [15].

As an aside, and by way of validation, it is noted that (10) can be derived by setting (68) equal to zero and solving for $a_s$. Furthermore, a solution can only be achieved here when $\pm \rightarrow -$ because $a_s \geq 0$ by definition. Using the negative sign corresponds to the minimum curve for $G_{Ct}$ when JSR $> JSR_c$, thereby demonstrating that the JSR must at least be greater than $JSR_c$ for the apparent target to be limited to one side of the cross-eye jammer.

## IV. DISCUSSION

The implications of each of the results derived in Section III are considered below for the following scenario whose parameters are representative of a missile engaging an aircraft or ship [10], [15]:

- X-Band radar (frequency is 10 GHz),
- 10° radar beamwidth ($d_r = 2.54$ wavelengths, and each radar antenna element is a uniformly excited aperture 2.54 wavelengths long),
- 1 km jammer range ($r = 1\,000$ m),
- 10 m jammer element separation ($d_c = 10$ m),
- 30° jammer rotation ($\theta_c = 30°$), and
- jammer amplitude and phase differences of 0.5 dB and 175° respectively ($a = 0.9441$ and $\phi = 175°$)

unless otherwise stated.

### A. Extreme Values

A number of extreme indicated-angle values obtained using (2) and (3) with the extreme total cross-eye gain values from (68) are shown in Figs 3(a) and 3(b) for amplitude mismatches of 0.5 dB ($a = 0.9441$) and 1 dB ($a = 0.8414$) respectively. The sum-channel 3-dB
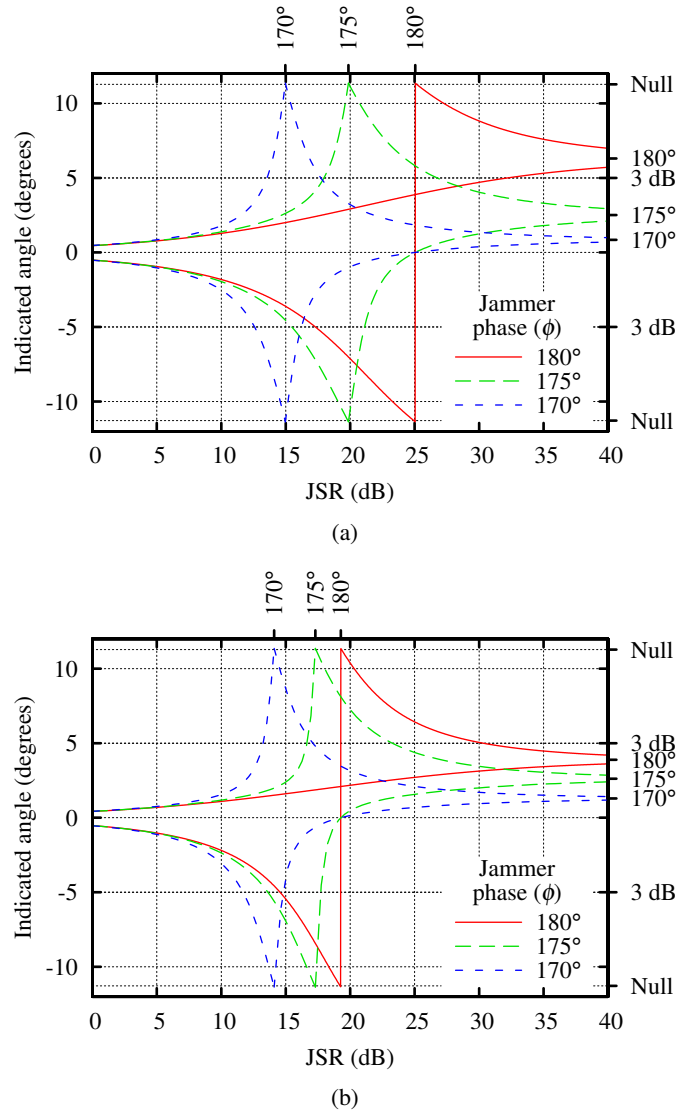


Fig. 3. The indicated angle as a function of JSR and $\phi$ for the case described in the text with the (a) $a = -0.5$ dB and (b) $a = -1.0$ dB.

antenna beamwidths, the positions of the first sum-channel nulls, and the indicated angles for the jammer alone are indicated on the right axes, and the critical JSR values are indicated on the top axes.

The first important observation is that the curves in Fig. 3 are identical to the corresponding curves which were published previously on the basis of $10^6$ computations of indicated angle over the full 360° range of $\phi_s$ values [15].

The values of $JSR_c$ are seen to correspond to the largest cross-eye gain ($G_{Ct}$) variation as infinite cross-eye gains are possible at $JSR_c$ as outlined in Section III. Equation (3) shows that an infinite cross-eye gain leads to an infinite monopulse ratio ($M_t$), and (2) means that an infinite monopulse ratio corresponds to an apparent target at first null of the sum-channel as shown in Fig. 3.

Increasing the jammer amplitude mismatch from

0.5 dB in Fig. 3(a) to 1 dB in Fig. 3(b) leads to a number of differences. The jammer sum-channel return is greater with a larger mismatch, so a lower JSR is required for the jammer and platform skin returns to be equal.

Also noticeable in Fig. 3 is the fact that the points where the minimum indicated angle is zero (implying that the minimum value of $G_{Ct} = 0$ by (2) and (3)) are very similar for all the cases considered. As outlined previously [16], this is a result of the fact that the approximation

$$\cos (\phi) \approx -1 \qquad (75)$$

is extremely accurate over the range of angles considered. There is thus only a weak dependence on $\phi$, so the points where the minimum value of $G_{Ct} = 0$ are expected to be close together. Using (75) allows (10) and (11) to the rewritten as

$$a_s \lessgtr 1 - a \qquad (76)$$
$$\text{JSR} \gtrless (1 - a)^{-2} \qquad (77)$$
$$\gtrless \text{JSR}_{c\,180} \qquad (78)$$

where the approximations are extremely accurate when $\phi \approx 180°$ (the design goal for a cross-eye jammer [15], [19]).

It is worth reiterating that Approximation 4 means that the exact value of $\text{JSR}_c$ is subject to error as noted in Section II. However, the main effect of the approximation is a JSR offset. Furthermore, this offset is less than 1.5 dB for the largest practical jammer-antenna separation of 20 m ($d_c = 20$ m) at the short range of 1 km ($r = 1000$ m) against a radar with a narrow beamwidth of only $2°$ ($d_r = 12.7$ wavelengths)[4], so the computed value of $\text{JSR}_c$ is sufficiently accurate to be useful in practical cross-eye jamming scenarios.

### B. Cross-Eye Gain Distribution

The cross-eye gain distributions obtained using (2), (3) and (64) for amplitude mismatches of 0.5 dB and 1 dB are shown in Fig. 4.

As for Fig. 3, the curves in Fig. 4 are identical to the corresponding curves which were published previously on the basis of $10^6$ computations of indicated angle over the full $360°$ range of $\phi_s$ values [15].

The main difference between plots in Fig. 4 is that the jammer sum-channel return given by $1 + a^2 + 2a \cos (\phi)$ is 1.8 times greater for Fig. 4(b) than for Fig. 4(a). Despite this large difference in jammer sum-channel return, the cross-eye gain values in the absence of platform skin return ($\text{JSR} \rightarrow \infty$ giving $a_s = 0$) are very similar, being

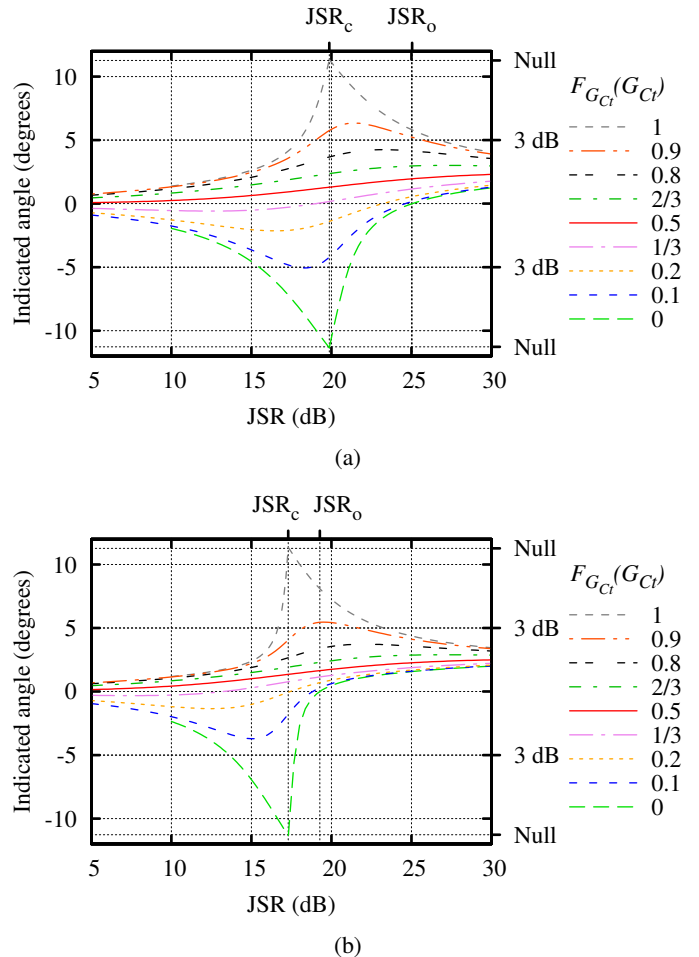[4]Missiles usually have a beamwidth on the order of $10°$.



Fig. 4. Total cross-eye gain which is below the specified cumulative probability values for the case described in the text with (a) $a = -0.5$ dB and (b) $a = -1$ dB.

11.05 for Fig. 4(a) and 10.54 for Fig. 4(b) (a difference of less than 5%). Despite this small difference in the absence of platform skin return, significant differences are seen when the effect of platform skin return is significant.

The first implication of the different jammer sum-channel return magnitudes is that larger JSR values are required to achieve given performance goals. For example, the jammer sum-channel return is equal to the skin sum-channel return at a JSR value ($\text{JSR}_c$) which is more than 2.5 dB lower for Fig. 4(b) ($\text{JSR}_c = 17.30$ dB) than for Fig. 4(a) ($\text{JSR}_c = 19.87$ dB). Furthermore, the JSR required to limit the indicated angles to positive values ($\text{JSR}_o$) is over 5.7 dB lower for Fig. 4(b) ($\text{JSR}_o = 19.27$ dB) than for Fig. 4(a) ($\text{JSR}_o = 25.05$ dB).

The second significant effect of the different jammer sum-channel return magnitudes is that the variation in the results is lower in Fig. 4(b) as can be seen in a number of ways. Firstly, the maximum values of the curves above the median ($F_{G_{Ct}} (G_{Ct}) > 0.5$) are larger in Fig. 4(a)
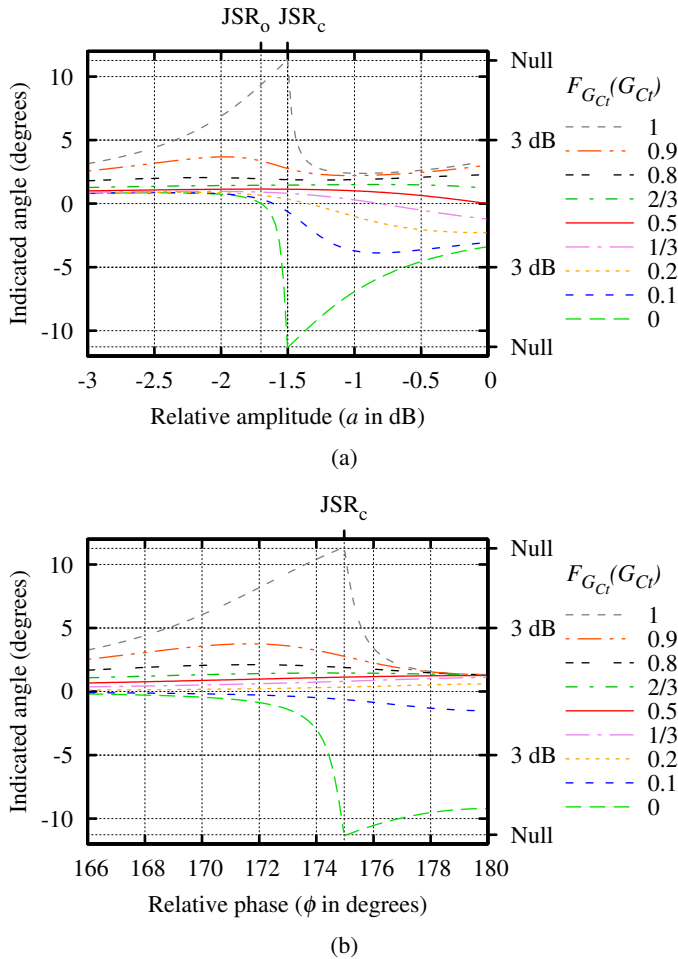
Fig. 5. Total cross-eye gain which is below the specified cumulative probability values for the case described in the text for a JSR of 15 dB (a) $\phi = -175°$ and (b) $a = -1.5$ dB.

than in Fig. 4(b), and a comparable observation holds for the curves below the median. This shows that the total cross-eye gain values are more closely clustered around the median value when the jammer sum-channel return is larger. Secondly, the curves in Fig. 4(a) are broader than in Fig. 4(b), showing that the skin return has a significant effect on the results over a greater range of JSR values. This is perhaps most clearly seen by the fact that difference between $JSR_o$ and $JSR_c$ is almost 5.2 dB for Fig. 4(a), but less than 2 dB for Fig. 4(b). The main implication of these observations are that a given improvement in JSR will have a greater effect when the jammer sum-channel return is greater.

Fig. 5 provides an alternative view of the total cross-eye gain distribution by plotting the results as a function of the jammer amplitude and phase mismatches ($a$ and $\phi$ respectively) for a fixed JSR of 15 dB. Both graphs in Fig. 5 are symmetrical about their right axes.

The general form of the graphs in Fig. 5 is similar to those in Fig. 4, but with the horizontal axis flipped.

This is a result of the fact that improving the matching between the two jammer channels ($a \rightarrow 0$ dB and $\phi \rightarrow 180°$) decreases the total jammer sum-channel return, and thus has a similar effect to increasing the JSR for fixed jammer parameters. Increasing the JSR would reduce the effect of skin return and thus cause the position of $JSR_c$ to move to the right in both graphs in Fig. 5.

Both the graphs in Fig. 5 have $JSR > JSR_c$ on the left, changing to $JSR < JSR_c$ on the right. This will not always be the case, as choosing an appropriate value of $\phi$ for Fig. 5(a) or $a$ for Fig. 5(b) would ensure that $JSR > JSR_c$ over the entire range of parameters considered.

The total jammer sum-channel return is far smaller at the right of Fig. 5(a) (0.00761) than at the right of Fig. 5(b) (0.02516) as a result of worse overall matching ($a = -1.5$ dB, $\phi = 180°$ versus $a = 0$ dB, $\phi = 175°$). The effect of this difference is most clearly seen by the fact that the median indicated angle increases significantly as the mismatch increases in Fig. 5(a), while a much smaller variation is observed in Fig. 5(b).

While the median total cross-eye gain ($G_{Ctm}$) increases as the jammer amplitude mismatch increases to the left of Fig. 5(a), the median cross-eye gain actually slightly decreases as the phase mismatch increases to the left of Fig. 5(b). The former case is due to the increasing total jammer sum-channel return as outlined above, while the latter case is due to the fact that cross-eye jamming is less effective when the matching between the jammer paths is far from 180° (e.g. [1]–[6], [8]). The effect of the total jammer sum-channel return and the performance of the cross-eye jammer thus need to be considered together to obtain a complete understanding of the effect of platform skin return on cross-eye jamming.

The fact that $JSR_o$ does not have a strong dependence on $\phi$ is borne out by Fig. 5(b) where the minimum total cross-eye gain is less than 0 for the full range of parameters shown. Additionally, all the values greater than the median have similar values to the median case when $\phi \approx 180°$ in Fig. 5(b). The fact that $JSR < JSR_c$ at this point is the reason that the upper half of the distribution tends to the median, while the opposite would be true if $JSR > JSR_c$. Both these observations echo those of previously-published work [15], [16], thereby providing additional validation of the results.

Fig. 6 shows the probability that a cross-eye jammer with the specified parameters will exceed the indicated angle on the bottom-right axis ($\theta_i$) for jammer amplitude mismatches of 0.5 dB and 1 dB respectively. The results were obtained using (2), (3) and (59).

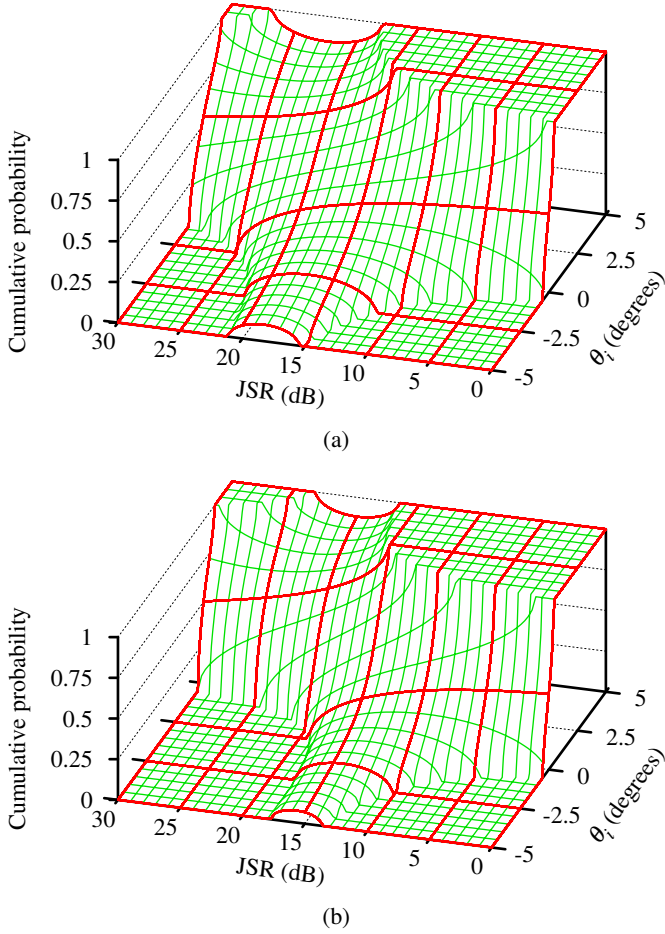In each case, the distribution develops a tail of nega-

Fig. 6. The cumulative probability as a function of the indicated angle for the case described in the text with (a) $a = -0.5$ dB and (b) $a = -1$ dB.

tive indicated angles (negative $G_{Ct}$) as the JSR increases. This negative tail is gradually replaced by a tail of positive indicated angles (positive $G_{Ct}$) as the JSR increases further. The tails for both positive and negative indicated angles stretch to the edge of the sum-channel main beam nulls when the sum-channel jammer and skin returns are equal ($JSR_c = 19.87$ dB and $17.30$ dB in Figs 6(a) and 6(b) respectively) as highlighted in Section IV-A.

The distributions for the two cases are almost identical when the JSR is 0 dB as the skin return dominates the result at this point. However, the two sets of distributions display increasingly pronounced differences as the JSR increases and the jammer has a greater effect. This general trend is anticipated as the skin returns in the two cases are identical, while the isolated jammer returns differ markedly.

The smaller total sum-channel jammer return in Fig. 6(a) leads to wider distributions than those in Fig. 6(b), as shown by the flatter curves in Fig. 6(a). For example, the curve at $JSR_c$ in Fig. 6(a) (effectively the 20-dB JSR curve) is much flatter than the corresponding

curve in Fig. 6(b) (slightly above the 17-dB JSR curve) indicating a significantly wider distribution. This distribution difference is especially important when there is a large distribution tail on the opposite side of the jammer to the desired apparent target [16].

However, the width of the distribution is not the only consideration, and (9) can be used to show that the median total cross-eye gain ($G_{Ctm}$) is greater in Fig. 6(a) than in Fig. 6(b) when the JSR is 26.5 dB or greater. While such a high JSR value may appear unrealistic, the reduced radar cross section (RCS) of modern platforms combined with the high effective isotropic radiated power (EIRP) of newer jammers mean that high JSR values are possible.

These observations clearly demonstrate the importance of considering the entire $G_{Ct}$ distribution rather than just the median or extreme values as was done in [15], or a single value as was done in [16].

Figs 7(a) and 7(b) plot the probability of exceeding a specified $G_{Ct}$ of 5 ($F_{G_{Ct}}(5)$) for JSR values of 15 dB and 20 dB respectively. The values shown on the graph are the probability of exceeding the specified cross-eye gain, so for example, the curve labelled "0.4" in Fig. 7(b) corresponds to a 40% probability of exceeding the a total cross-eye gain of 5. As in the contour plots published previously, the values are symmetrical around $a = 0$ dB, with the only difference being the side of the jammer on which the false target is produced.

The contours in Fig. 7 are symmetrical around $\phi = 180°$. This is a result of the fact that the only dependence on $\phi$ in the main results in Section III is of the from $\cos(\phi)$, which is symmetrical around $\phi = 180°$.

Fig. 7 is similar to the relevant plots in other works (e.g. [15], [19]), but with the notable difference that contours of constant probability are shown in Fig. 7, while other published results show contours of constant cross-eye gain. This change makes the contour plots in Fig. 7 far more useful than the previously-published results in [15] because only consider the median case was considered. As a result, only the curves labelled "0.5" can be obtained based on the analysis in [15].

The tolerance requirements become stricter (the areas within the contours become smaller) as the proportion of possible $G_{Ct}$ values below the specified value decreases. This result is anticipated because a smaller value of $F_{G_{Ct}}(G_{Cts})$ means that more solutions exceed $G_{Cts}$, leading to higher cross-eye gain values, and thus tighter tolerances [19].

The contours in Fig. 7(b) are significantly larger than the corresponding contours in Fig. 7(a) due to the greater JSR in Fig. 7(b) leading to a stronger jammer return. This stronger jammer return reduces the effect of skin return,
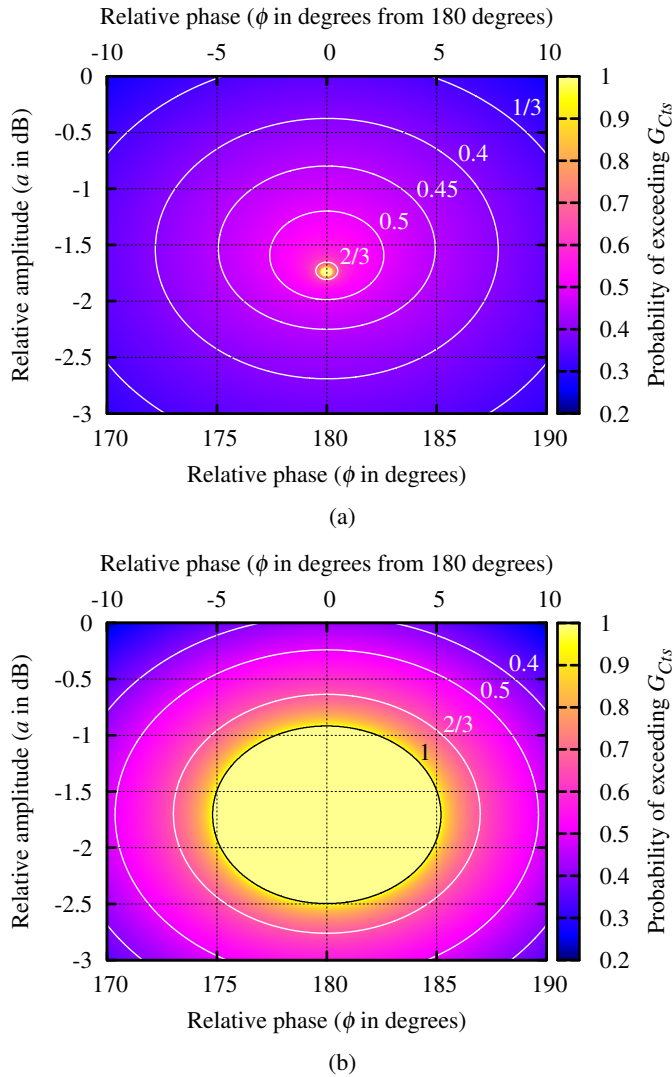
(a)



(b)

Fig. 7. Probability that the total cross-eye gain will exceed 5 for JSR values of (a) 15 dB and (b) 20 dB.

leading to smaller $G_{Ct}$ variations as a result of platform skin-return phase.

## V. Conclusion

An understanding of how platform skin return affects the operation of a retrodirective cross-eye jammer is of significant practical interest. Unfortunately, published results which consider this scenario suffer from a number of deficiencies which limit their value.

A mathematically-rigorous derivation of the distribution of the total cross-eye gain which results from skin-return affected retrodirective cross-eye jamming has been provided. The mathematical rigour addresses limitations of previous analyses, and the closed-form solutions obtained allow extensive analysis of the effects of platform skin return on retrodirective cross-eye jamming.

A number of examples of how the new results can be applied have been presented, with the main conclusion

being that the problem as must be considered a whole. For example, the effect of mismatching the two paths through a retrodirective cross-eye jammer serves to decrease the effect of skin return by increasing the sum-channel return of the jammer as a whole. However, these same changes reduce the effectiveness of the cross-eye jammer when considered in isolation. The result is that compromises between the conflicting goals of decreasing the effect of skin return with greater mismatches and obtaining higher jammer performance through improved matching must be made. The results provided allow such analyses to be performed by providing a complete description of retrodirective cross-eye jamming in the presence of platform skin return.

## References

[1] P. E. Redmill, "The principles of artificial glint jamming ("cross eye")," Royal Aircraft Establishment (Farnborough), Tech. note RAD. 831, March 1963.

[2] L. B. Van Brunt, *Applied ECM*. EW Engineering, Inc., 1978, vol. 1.

[3] A. Golden, *Radar Electronic Warfare*. AIAA Inc., 1987.

[4] D. C. Schleher, *Electronic warfare in the information age*. Artech House, 1999.

[5] D. L. Adamy, *EW 101: A first course in electronic warfare*. Artech House, 2001.

[6] F. Neri, *Introduction to Electronic Defense Systems*, 2nd ed. SciTech Publishing, 2006.

[7] L. Falk, "Cross-eye jamming of monopulse radar," in *IEEE Waveform Diversity & Design Conf.*, 4-8 June 2007, pp. 209–213.

[8] W. P. du Plessis, "A comprehensive investigation of retrodirective cross-eye jamming," Ph.D. dissertation, University of Pretoria, 2010.

[9] L. C. Van Atta, "Electromagnetic reflector," U.S.A. Patent 2 908 002, Oct. 6, 1959.

[10] W. P. du Plessis, J. W. Odendaal, and J. Joubert, "Extended analysis of retrodirective cross-eye jamming," *IEEE Trans. Antennas Propag.*, vol. 57, no. 9, pp. 2803–2806, Sept. 2009.

[11] W. P. du Plessis, J. W. Odendaal, and J. Joubert, "Experimental simulation of retrodirective cross-eye jamming," *IEEE Trans. Aerosp. Electron. Syst.*, vol. 47, no. 1, pp. 734–740, Jan. 2011.

[12] G. E. Johnson, "Jamming passive lobing radars," *Electronic Warfare*, vol. 9, pp. 75–85, April 1977.

[13] R. N. Lothes, M. B. Szymanski, and R. G. Wiley, *Radar vulnerability to jamming*. Artech House, 1990.

[14] Y. Stratakos, G. Geroulis, and N. Uzunoglu, "Analysis of glint phenomenon in a monopulse radar in the presence of skin echo and non-ideal interferometer echo signals," *J. Electromagn. Waves Appl.*, vol. 19, no. 5, pp. 697–711, 2005.

[15] W. P. du Plessis, "Platform skin return and retrodirective cross-eye jamming," *IEEE Trans. Aerosp. Electron. Syst.*, vol. 48, no. 1, pp. 490–501, Jan. 2012.

[16] W. P. du Plessis, "Limiting apparent target position in skin-return influenced cross-eye jamming," *IEEE Trans. Aerosp. Electron. Syst.*, vol. 49, no. 3, pp. 2097–2101, July 2013.

[17] S. M. Sherman and D. K. Barton, *Monopulse principles and techniques*, 2nd ed. Artech House, 2011.

[18] W. P. du Plessis, "Modelling monopulse antenna patterns," in *Saudi Int. Electron. Commun. Photon. Conf. (SIECPC)*, 27-30 April 2013, pp. 1–5.

[19] W. P. du Plessis, J. W. Odendaal, and J. Joubert, "Tolerance analysis of cross-eye jamming systems," *IEEE Trans. Aerosp. Electron. Syst.*, vol. 47, no. 1, pp. 740–745, Jan. 2011.

[20] M. R. Spiegel and J. Liu, *Mathematical Handbook of Formulas and Tables*, 2nd ed., ser. Schaum's Outline Series. McGraw-Hill, 1999.

**Warren du Plessis** (M'00, SM'10) received the B.Eng. (Electronic) and M.Eng. (Electronic) and Ph.D. (Engineering) degrees from the University of Pretoria in 1998, 2003 and 2010 respectively, winning numerous academic awards including the prestigious Vice-Chancellor and Principal's Medal.

He spent two years as a lecturer at the University of Pretoria, and then joined Grintek Antennas as a design engineer for almost four years, followed by six years at the Council for Scientific and Industrial Research (CSIR). He is currently an Associate Professor at the University of Pretoria, and his primary research interests are cross-eye jamming and thinned antenna arrays.